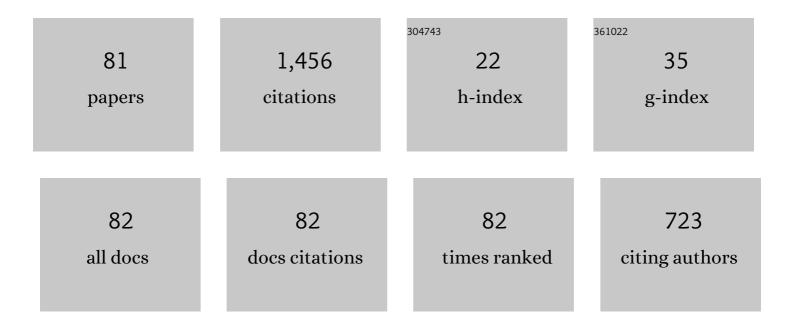
List of Publications by Year in descending order

Source: https://exaly.com/author-pdf/3551868/publications.pdf Version: 2024-02-01



TOMOVA NACIDA

#	Article	IF	CITATIONS
1	Development of X-ray Imaging for Observing Solidification of Carbon Steels. ISIJ International, 2011, 51, 402-408.	1.4	100
2	Granular deformation mechanisms in semi-solid alloys. Acta Materialia, 2011, 59, 4933-4943.	7.9	89
3	<i>In situ</i> observation of solidification phenomena in Al–Cu and Fe–Si–Al alloys. International Journal of Cast Metals Research, 2009, 22, 15-21.	1.0	81
4	Direct observation of deformation in semi-solid carbon steel. Scripta Materialia, 2011, 64, 1129-1132.	5.2	81
5	In situ investigation of unidirectional solidification in Sn–0.7Cu and Sn–0.7Cu–0.06Ni. Acta Materialia, 2011, 59, 4043-4054.	7.9	56
6	Evaluation of dynamic development of grain structure during friction stir welding of pure copper using a quasi in situ method. Journal of Materials Science and Technology, 2019, 35, 1412-1421.	10.7	56
7	Thermoelectric properties of (Na1â^'yMy)xCo2O4 (M=K, Sr, Y, Nd, Sm and Yb; y=0.01â^¼0.35). Journal of Alloys and Compounds, 2003, 348, 263-269.	5.5	52
8	<i>In situ</i> observation of nucleation, fragmentation and microstructure evolution in Sn–Bi and Al–Cu alloys. International Journal of Cast Metals Research, 2008, 21, 125-128.	1.0	48
9	Experimental evaluation of strain and strain rate during rapid cooling friction stir welding of pure copper. Science and Technology of Welding and Joining, 2019, 24, 352-359.	3.1	47
10	Dilatancy in semi-solid steels at high solid fraction. Acta Materialia, 2017, 125, 187-195.	7.9	40
11	Massive transformation from <i>Î′</i> phase to <i>γ</i> phase in Fe–C alloys and strain induced in solidifying shell. IOP Conference Series: Materials Science and Engineering, 2012, 33, 012036.	0.6	38
12	Real time synchrotron X-ray observations of solidification in hypoeutectic Al–Si alloys. Materials Characterization, 2013, 85, 134-140.	4.4	34
13	In situ study of granular micromechanics in semi-solid carbon steels. Acta Materialia, 2013, 61, 4169-4179.	7.9	34
14	Investigation of temperature dependent microstructure evolution of pure iron during friction stir welding using liquid CO2 rapid cooling. Materials Characterization, 2018, 137, 24-38.	4.4	33
15	Microstructure evolution of Cu–30Zn during friction stir welding. Journal of Materials Science, 2018, 53, 10423-10441.	3.7	31
16	Impact of melt convection induced by ultrasonic wave on dendrite growth in Sn–Bi alloys. Materials Letters, 2015, 150, 135-138.	2.6	30
17	Effect of Stacking Fault Energy on the Grain Structure Evolution of FCC Metals During Friction Stir Welding. Acta Metallurgica Sinica (English Letters), 2020, 33, 1001-1012.	2.9	30
18	Influence of Mg on Solidification of Hypereutectic Cast Iron: X-ray Radiography Study. Metallurgical and Materials Transactions A: Physical Metallurgy and Materials Science, 2015, 46, 4937-4946.	2.2	28

#	Article	IF	CITATIONS
19	Effect of Partial Substitution of 3d Transition Metals for Co on the Thermoelectric Properties of Na <sub>x</sub> Co <sub>2</sub> O <sub>4</sub> . Materials Transactions, 2002, 43, 601-604.	1.2	25
20	In-situobservation of peritectic solidification in Sn-Cd and Fe-C alloys. IOP Conference Series: Materials Science and Engineering, 2012, 27, 012084.	0.6	25
21	Strain rate dependent micro-texture evolution in friction stir welding of copper. Materialia, 2019, 6, 100302.	2.7	23
22	Semi-solid deformation of Al-Cu alloys: A quantitative comparison between real-time imaging and coupled LBM-DEM simulations. Acta Materialia, 2019, 163, 208-225.	7.9	23
23	Characterization of Shear Deformation Based on In-situ Observation of Deformation in Semi-solid Al–Cu Alloys and Water-particle Mixture. ISIJ International, 2013, 53, 1195-1201.	1.4	21
24	Thermoelectric properties of NaxCo2O4 with rare-earth metals doping prepared by polymerized complex method. Journal of Alloys and Compounds, 2006, 408-412, 1217-1221.	5.5	19
25	Kinetics of the $\hat{l}' \hat{l}^3$ interface in the massive-like transformation in Fe-0.3C-0.6Mn-0.3Si alloys. IOP Conference Series: Materials Science and Engineering, 2015, 84, 012062.	0.6	19
26	Interface Energies of Hetero- and Homo-Phase Boundaries and Their Impact on δ-γ Massive-Like Phase Transformations in Carbon Steel. Materials Transactions, 2015, 56, 1461-1466.	1.2	18
27	In Situ Observation of Deformation in Semi-solid Fe-C Alloys at High Shear Rate. Metallurgical and Materials Transactions A: Physical Metallurgy and Materials Science, 2014, 45, 5613-5623.	2.2	17
28	Concurrent γ-Phase Nucleation as a Possible Mechanism of δ-γ Massive-like Phase Transformation in Carbon Steel: Numerical Analysis Based on Effective Interface Energy. Materials Transactions, 2015, 56, 1467-1474.	1.2	17
29	Synthesis of NaxCo2O4thermoelectric oxide with crystallographic anisotropy by chemical solution process. Science and Technology of Advanced Materials, 2004, 5, 125-131.	6.1	16
30	Nucleation and Growth in Undercooled Melts of Bulk-Metallic-Glass Forming Zr <sub>60</sub> Ni <sub>25</sub> Al <sub>15</sub> Alloy. Materials Transactions, 2005, 46, 2762-2767.	1.2	14
31	Effect of the Melt Flow on the Solidified Structure of Middle Carbon Steel by Means of the Levitation Method Using Alternating and Static Magnetic Fields. ISIJ International, 2007, 47, 612-618.	1.4	14
32	Time-resolved and <i>In-situ</i> Observation of δ-γ Transformation during Unidirectional Solidification in Fe-C Alloys. Tetsu-To-Hagane/Journal of the Iron and Steel Institute of Japan, 2019, 105, 290-298.	0.4	14
33	Mechanism of grain structure development for pure Cu and Cu-30Zn with low stacking fault energy during FSW. Science and Technology of Welding and Joining, 2020, 25, 669-678.	3.1	14
34	Effect of the Polymerized Complex Process on Doping Limit of Thermoelectric Na <i><sub>x</sub></i> Co <sub>1−<i>y</i></sub> M <i><sub>y</sub></i> O <sub>2</sub> (M=Mn,)	Tj <b>£⊉</b> Qq0(	D <b>Q.3</b> gBT /Ove
35	Three-dimensional alignment of FeSi <sub>2</sub> with orthorhombic symmetry by an anisotropic magnetic field. Journal of Physics: Conference Series, 2009, 165, 012021.	0.4	13

36Chain structure in the unidirectionally solidified Al2O3â€"YAGâ€"ZrO2 eutectic composite. Journal of<br/>Crystal Growth, 2009, 311, 3765-3770.1.513

#	Article	IF	CITATIONS
37	Synchrotron Radiography Studies of Shear-Induced Dilation in Semisolid Al Alloys and Steels. Jom, 2014, 66, 1415-1424.	1.9	13
38	Selection of the Massive-like <i>Î </i> - <i>Î 3</i> Transformation due to Nucleation of Metastable <i>Î </i> Phase in Fe-18 Mass%Cr-Ni Alloys with Ni Contents of 8, 11, 14 and 20 Mass%. ISIJ International, 2019, 59, 459-465.	1.4	13
39	Time-resolved X-ray imaging of solidification cracking for Al-Cu alloy at the weld crater. Materials Characterization, 2020, 167, 110469.	4.4	13
40	In situ observation of solidification crack propagation for type 310S and 316L stainless steels during TIG welding using synchrotron X-ray imaging. Journal of Materials Science, 2021, 56, 10653-10663.	3.7	12
41	Microstructural Evolutions of 2N Grade Pure Al and 4N Grade High-Purity Al during Friction Stir Welding. Materials, 2021, 14, 3606.	2.9	12
42	Thermoelectric Properties of Na <sub>x</sub> Co <sub>2</sub> O <sub>4</sub> Prepared by the Polymerized Complex Method and Spark Plasma Sintering. Materials Transactions, 2003, 44, 1866-1871.	1.2	11
43	Effect of Partial Substitutions of Rare-earth Metals for Na-site on the Thermoelectric Properties of Na <sub><i>x</i></sub> Co <sub>2</sub> O <sub>4</sub> Prepared by the Polymerized Complex Method. Materials Transactions, 2004, 45, 1339-1345.	1.2	11
44	Flowering of Continuous Casting Process for Steel in Japan and New Fundamental Seeds to the Future. Tetsu-To-Hagane/Journal of the Iron and Steel Institute of Japan, 2014, 100, 472-484.	0.4	10
45	Impacts of Interface Energies and Transformation Strain from BCC to FCC on Massive-like δ-γ Transformation in Steel. IOP Conference Series: Materials Science and Engineering, 2015, 84, 012049.	0.6	10
46	Synchrotron radiography of direct-shear in semi-solid alloys. IOP Conference Series: Materials Science and Engineering, 2012, 27, 012086.	0.6	9
47	Microstructure and Thermoelectric Properties of NaxCo2O4 Synthesized by Spark Plasma Sintering Funtai Oyobi Fummatsu Yakin/Journal of the Japan Society of Powder and Powder Metallurgy, 2002, 49, 406-411.	0.2	8
48	Solidification of Al2O3–YAG eutectic composites with off-metastable eutectic composition from undercooled melt produced by melting Al2O3–YAP eutectics. Journal of the European Ceramic Society, 2012, 32, 2137-2143.	5.7	7
49	Role of annealing twinning in microstructural evolution of high purity silver during friction stir welding. Science and Technology of Welding and Joining, 2019, 24, 644-651.	3.1	7
50	Thermoelectric Properties of Na <sub>x</sub> Co <sub>2</sub> O <sub>4</sub> Prepared by the Polymerized Complex Method and Hot-Pressing. Materials Transactions, 2003, 44, 155-160.	1.2	6
51	<i>In-situ</i> Measurement of Solute Partition Coefficient in Fe-Cr-Ni-Mo Alloys by Using X-ray Imaging and X-ray Florescence Analysis. Tetsu-To-Hagane/Journal of the Iron and Steel Institute of Japan, 2017, 103, 678-687.	0.4	6
52	Direct observation of solidification behaviors of Fe-Mn-Si alloys during TIG spot welding using synchrotron X-ray. Scripta Materialia, 2022, 216, 114743.	5.2	6
53	Effects of Shaping Conditions on the Microstructure and the Mechanical Property of the Al <sub>2</sub> O <sub>3</sub> -YAG Eutectic Composite Produced by Melting the Al <sub>2</sub> O <sub>3</sub> -YAP Eutectic Structure. Materials Transactions, 2007, 48, 2312-2315.	1.2	5
54	Formation and microstructure of Al <sub>2</sub> O <sub>3</sub> -YAG eutectic ceramics by phase transformation from metastable system to equilibrium system. Journal of Physics: Conference Series, 2009, 165, 012006.	0.4	5

#	Article	IF	CITATIONS
55	Macroscopic modelling of semisolid deformation for considering segregation bands induced by shear deformation. IOP Conference Series: Materials Science and Engineering, 2012, 33, 012053.	0.6	5
56	Yet Another Marked Difference among Impurities as Modifier Elements for Refinement of Eutectic Si in Al-Si Alloys. Materials Transactions, 2015, 56, 1475-1483.	1.2	5
57	<i>In Situ</i> Observations of Tensile and Compressive Deformations in Semi Solid Metallic Alloys Using Time-resolved X-ray Imaging. Tetsu-To-Hagane/Journal of the Iron and Steel Institute of Japan, 2017, 103, 668-677.	0.4	5
58	X-Ray Imaging of Formation and Growth of Spheroidal Graphite in Ductile Cast Iron. Materials Science Forum, 2018, 925, 104-109.	0.3	5
59	Time-resolved and <i>In-situ</i> Observation of <i>δ</i> – <i>γ</i> Transformation during Unidirectional Solidification in Fe–C Alloys. ISIJ International, 2020, 60, 930-938.	1.4	5
60	Friction Stir Welding of High Phosphorus Weathering Steel– Weldabilities, Microstructural Evolution and Mechanical Properties. Tetsu-To-Hagane/Journal of the Iron and Steel Institute of Japan, 2020, 106, 892-901.	0.4	5
61	Regular Structure Formation of Hypermonotectic Al-In Alloys. Materials Science Forum, 2010, 649, 131-136.	0.3	4
62	Fabrication of Al <sub>2</sub> 0 <sub>3</sub> –YAC Equilibrium Eutectic Composites via Transformation from Fine Al <sub>2</sub> 0 <sub>3</sub> and YAP Powder Mixtures. Materials Transactions, 2012, 53, 1124-1129.	1.2	4
63	Influences of temperature and Sn-addition on microstructural evolution of Ag during FSW. Science and Technology of Welding and Joining, 2020, 25, 198-207.	3.1	4
64	Microstructural Control and Development of Synthesis Route for Enhancing Performance of Sintered Thermoelectric Oxide Polycrystals via Chemical Solution Process. Funtai Oyobi Fummatsu Yakin/Journal of the Japan Society of Powder and Powder Metallurgy, 2010, 57, 224-231.	0.2	3
65	放å°,,å‰ã,'å^©ç"¨ã⊷ãŸã,¢ãƒ«ãƒŸãƒ‹ã,¦ãƒå•́金ã®å‡å›°ç¾è±jã®è§£æ~Ž. Keikinzoku/Journal of Japan Instit	ute@f4Ligł	nt Mætals, 20
66	<i>In situ</i> Observation of Dendrite Growth in Sn-Bi Alloys under Ultrasonic Vibration Using Time-resolved X-ray Imaging. Tetsu-To-Hagane/Journal of the Iron and Steel Institute of Japan, 2016, 102, 170-178.	0.4	3
67	Erratum to "Selection of the Massive-like <i>δ</i> - <i>γ</i> Transformation due to Nucleation of Metastable <i>δ</i> Phase in Fe-18 Mass%Cr-Ni Alloys with Ni Contents of 8, 11, 14 and 20 Mass%―[ISIJ International, Vol. 59 (2019), No. 3, pp. 459-465]. ISIJ International, 2021, 61, 1053-1053.	1.4	2
68	Development in In Situ Observation of Deformation in Semi-solid Alloys Using X-Ray Imaging. , 2014, , 231-243.		2
69	Characterization of Shear Deformation Based on In-situ Observation of Deformation in Semi-Solid Al-Cu Alloys and Water-Particle Mixture. Tetsu-To-Hagane/Journal of the Iron and Steel Institute of Japan, 2013, 99, 141-148.	0.4	2
70	Thermoelectric Properties of (Na1-yMy)xCo2O4 (M: K, Sr, Y, Nd, Sm and Yb; y = 0.01â‰^0.35) ChemInform, 2003, 34, no.	0.0	1
71	Crystal growth in the bulk-metallic-glass Zr-based alloys by using the DC + AC levitation method. Journal of Physics: Conference Series, 2009, 144, 012056.	0.4	1
72	Direct Observation of Shear Deformation in Semi-solid Alloys Using X-ray Imaging. Materia Japan, 2012, 51, 561-568.	0.1	1

#	Article	IF	CITATIONS
73	Localization of shear strain and shear band formation induced by deformation in semi-solid Al-Cu alloys. IOP Conference Series: Materials Science and Engineering, 2015, 84, 012078.	0.6	1
74	Three-dimensional Observation of Al <sub>2</sub> O <sub>3</sub> -GAP Eutectic Structure by X-ray Micro CT. Materia Japan, 2007, 46, 819-819.	0.1	1
75	Thermoelectric properties of Na/sub x/Co/sub 2/O/sub 4/ prepared by the polymerized complex method. , 0, , .		0
76	SYNTHESIS OF NaxCo2O4 THERMOELECTRIC OXIDE BY THE POLYMERIZED COMPLEX METHOD AND SPS METHODS. , 2005, , 317-320.		0
77	<i>In Situ</i> Study of the Altering Globule Packing-Density during Semisolid Alloy Deformation. Solid State Phenomena, 0, 192-193, 185-190.	0.3	0
78	Advanced Analysis of Solidification by X-ray Imaging. , 2013, , 93-104.		0
79	In Situ Observation of Solidification Behaviors in Carbon Steels Using Synchrotron X-ray Imaging. Materia Japan, 2014, 53, 467-470.	0.1	0
80	Application of a macroscopic model to predict the band segregation induced by shear deformation of semisolid. IOP Conference Series: Materials Science and Engineering, 2015, 84, 012011.	0.6	0
81	In situ Observation Using Synchrotron Radiation. Yosetsu Gakkai Shi/Journal of the Japan Welding Society, 2019, 88, 274-278.	0.1	0